

NUMERICAL SIMULATION OF SHOCK WAVES IN BUBBLY LIQUIDS: A PRELIMINARY STUDY

KEH-MING SHYUE *

Abstract. We report preliminary results obtained using a fluid-mixture type multicomponent algorithm developed by the author for compressible two-phase flow with shock waves in liquids containing a small concentration of gas bubbles in two space dimensions. We demonstrate the well-known belief that the presence of gas bubbles in the liquid tends to make the waves dissipative and dispersive, depending on the strength of the incident shock wave. In this study, a stiffened gas equation of state is used to describe the basic thermodynamic behavior of the liquid, while a van der Waals equation of state is employed for the gas. The algorithm uses a hybrid version of the stiffened and van der Waals equations of state as a basis for the mixing between liquid and gas phases within a grid cell, and have a mixture type of the model equations for the motion of the fluids. A standard high-resolution method based on a wave-propagation viewpoint is used to solved the proposed system, giving an efficient implementation of the algorithm.

Key words: bubbly flow, multicomponent algorithm, shock wave, van der Waals gas

1. Introduction. The study of the propagation of pressure waves through a liquid containing many gas bubbles or solid suspensions is of fundamental importance in many field of engineering and sciences [3, 4, 8]. One typical problem of this kind is to see whether or not bubbles could be the principal factors in the effects on ship and submarine wakes on the propagation of sound, and so one is interested in the acoustic properties of gas bubbles in liquids (cf. [15]). In the other situations where the flow is in a transient operations of chemical process and is possibly undergone vapor explosions [14], the behavior of the waves in the induced bubbly media is in no doubt crucial to such an industrial problem. Besides the above mentioned technical applications, most importantly we are interested in finding fundamental mechanisms and so theory on the way to connect the properties of the microstructure (in this case the gas bubbles) with the macroscopic phenomena (like transport properties) of the problems.

It is clear that the class of problems considered here is of multiphase in nature, and the solutions of the governing systems may possess highly oscillatory or even chaotic modes in large part of the physical regions of practical interests. Standard solution techniques such as the direct numerical simulations and the methods of averaging (cf. [1, 2, 3]) are often used to construct approximate solutions of the problems at various situations. For some simple model problems, as in comparison with laboratory experiments, some agreement and disagreement of the theoretical results have been found and documented, see [16] for a review of the previous work. Since in general the microstructure of the gas bubbles has a very complicated substructure, up to now, we have not yet found any related results obtained by simulating the problem directly. It is our goal in this article to perform a benchmark test of shock waves in bubbly liquids using the recently developed multicomponent algorithm for general compressible flows [9, 10, 13], see Fig. 1.1 for a basic setup of the problem in two space dimensions. Detailed comparison with theoretical models and experiments of the problem will be considered in the future and reported in elsewhere [12].

*Department of Mathematics, National Taiwan University, Taipei, Taiwan 106, Republic of China (shyue@math.ntu.edu.tw).

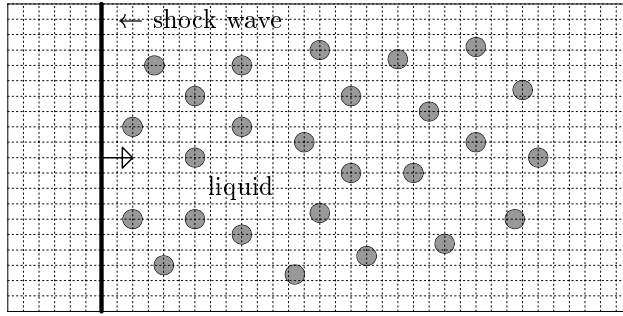


FIG. 1.1. A typical grid setup for the numerical simulations of two-phase flow problems with shock waves in bubbly liquids. It is those grid cells that are cut by the bubbles requiring special attentions for the proper numerical treatments. Note that the gas bubbles (the shaded regions) only occupy a small portion of the entire domain.

2. Two-Phase Flow Model. To best demonstrate the basic solution features of shock waves in bubbly liquids, we consider a two-dimensional flow, and use the Euler equations of gas dynamics as a model system for the motion of the liquid and gas,

$$\frac{\partial}{\partial t} \begin{pmatrix} \rho \\ \rho u \\ \rho v \\ \rho E \end{pmatrix} + \frac{\partial}{\partial x} \begin{pmatrix} \rho u \\ \rho u^2 + p \\ \rho uv \\ \rho Eu + pu \end{pmatrix} + \frac{\partial}{\partial y} \begin{pmatrix} \rho v \\ \rho uv \\ \rho v^2 + p \\ \rho Ev + pv \end{pmatrix} = 0, \quad (2.1)$$

where ρ is the density, u and v are the particle velocities in the x - and y -direction respectively, p is the pressure, and E is the specific total energy. To complete the system, in the liquid-phase part of the domain, we assume the fluid satisfies a stiffened gas equation of state,

$$p(\rho, e) = (\gamma - 1)\rho e - \gamma \mathcal{B}, \quad (2.2)$$

while in the gas-phase part of the domain, the fluid fulfills a van der Waals equation of state,

$$p(\rho, e) = \left(\frac{\gamma - 1}{1 - b\rho} \right) (\rho e + a\rho^2) - a\rho^2. \quad (2.3)$$

Here e denotes the specific internal energy, γ is the ratio of specific heats ($\gamma > 1$), \mathcal{B} is a pressure-like constant, and the quantities a , b are the van der Waals gas constants for molecular cohesive forces and the finite size of molecules, respectively ($a \geq 0$, $0 \leq b < 1/\rho$), see [6, 7] for numerical values to various gaseous or liquid substances. As usual we set $E = e + (u^2 + v^2)/2$. The four components of (2.1) express the conservation of mass, momenta in the x - and y -direction, and energy, respectively [5].

To deal with grid cell that contains more than one fluid component, in our multicomponent algorithm, we introduce a hybrid version of (2.2) and (2.3) of the form,

$$p(\rho, e) = \left(\frac{\gamma - 1}{1 - b\rho} \right) (\rho e - \mathcal{B} + a\rho^2) - (\mathcal{B} + a\rho^2), \quad (2.4)$$

to describe the basic thermodynamic behavior of the mixing between the two different liquid and gas phases. For the equations, we use an extended system that combines (2.1) for the motion of the conservative mixtures: ρ , ρu , ρv , and ρE , and the following set of equations for the material-dependent quantities: γ , a , b , and \mathcal{B} , appearing in (2.4),

$$\frac{\partial}{\partial t} \left(\frac{b\rho}{\gamma-1} \right) + \frac{\partial}{\partial x} \left(\frac{b\rho}{\gamma-1} u \right) + \frac{\partial}{\partial y} \left(\frac{b\rho}{\gamma-1} v \right) = 0, \quad (2.5a)$$

$$\begin{aligned} \frac{\partial}{\partial t} \left(\frac{\gamma-b\rho}{\gamma-1} \mathcal{B} \right) + \frac{\partial}{\partial x} \left(\frac{\gamma-b\rho}{\gamma-1} \mathcal{B} u \right) + \frac{\partial}{\partial y} \left(\frac{\gamma-b\rho}{\gamma-1} \mathcal{B} v \right) = \\ \left(\frac{\gamma}{\gamma-1} \mathcal{B} \right) \left(\frac{\partial u}{\partial x} + \frac{\partial v}{\partial y} \right), \end{aligned} \quad (2.5b)$$

$$\begin{aligned} \frac{\partial}{\partial t} \left(\frac{2-\gamma-b\rho}{\gamma-1} a\rho^2 \right) + \frac{\partial}{\partial x} \left(\frac{2-\gamma-b\rho}{\gamma-1} a\rho^2 u \right) + \\ \frac{\partial}{\partial y} \left(\frac{2-\gamma-b\rho}{\gamma-1} a\rho^2 v \right) = - \left(\frac{2-\gamma-2b\rho}{\gamma-1} a\rho^2 \right) \left(\frac{\partial u}{\partial x} + \frac{\partial v}{\partial y} \right), \end{aligned} \quad (2.5c)$$

$$\frac{\partial}{\partial t} \left(\frac{1}{\gamma-1} \right) + \frac{\partial}{\partial x} \left(\frac{1}{\gamma-1} u \right) + \frac{\partial}{\partial y} \left(\frac{1}{\gamma-1} v \right) = 0, \quad (2.5d)$$

$$\frac{\partial a}{\partial t} + u \frac{\partial a}{\partial x} + v \frac{\partial a}{\partial y} = 0. \quad (2.5e)$$

We note that the above equations, i.e., (2.5a)–(2.5e), are constructed in such a way that not only the pressure retains in equilibrium for an *interface only* mixture cell, but also the mass remains conserve on the entire domain, see [10] for the details. Having a system set in this way, there is no problem to compute the time-evolution of the pressure *via* the equation of state,

$$p = \left[\rho E - \frac{(\rho u)^2 + (\rho v)^2}{2\rho} - \left(\frac{b\rho}{\gamma-1} \mathcal{B} \right) - \left(\frac{2-\gamma-b\rho}{\gamma-1} a\rho^2 \right) \right] / \left(\frac{1-b\rho}{\gamma-1} \right). \quad (2.6)$$

It is clear that the proposed system of equations for the fluid mixtures is not written in the full conservation form, but is rather a combination of conservation and transport equations. Despite this, it is nevertheless a hyperbolic system of equations as it can be easily verified when formulating the system in a quasi-linear form

$$\frac{\partial q}{\partial t} + A(q) \frac{\partial q}{\partial x} + B(q) \frac{\partial q}{\partial y} = 0, \quad (2.7)$$

and determining the associated eigen-structure of the matrices A and B for each physically relevant values of q located in the region of thermodynamic stability (cf. [10]). Here the state vector q in the system is defined by

$$q = \left[\rho, \rho u, \rho v, \rho E, \frac{b\rho}{\gamma-1}, \frac{\gamma-b\rho}{\gamma-1} \mathcal{B}, \frac{2-\gamma-b\rho}{\gamma-1} a\rho^2, \frac{1}{\gamma-1}, a \right]^T,$$

and the matrices A and B are given by

$$A(q) = \begin{bmatrix} 0 & 1 & 0 & 0 & 0 & 0 & 0 & 0 & 0 \\ K - u^2 & u(2 - \Gamma) & -v\Gamma & \Gamma & p\Gamma & -\Gamma & -\Gamma & -p\Gamma & 0 \\ -uv & v & u & 0 & 0 & 0 & 0 & 0 & 0 \\ u(K - H) & H - u^2\Gamma & -uv\Gamma & u(\Gamma + 1) & up\Gamma & -u\Gamma & -u\Gamma & -up\Gamma & 0 \\ -\varphi u & \varphi & 0 & 0 & u & 0 & 0 & 0 & 0 \\ \varphi u\mathcal{B} & -\varphi\mathcal{B} & 0 & 0 & 0 & u & 0 & 0 & 0 \\ -\chi u & \chi & 0 & 0 & 0 & 0 & u & 0 & 0 \\ 0 & 0 & 0 & 0 & 0 & 0 & 0 & u & 0 \\ 0 & 0 & 0 & 0 & 0 & 0 & 0 & 0 & u \end{bmatrix}$$

and

$$B(q) = \begin{bmatrix} 0 & 0 & 1 & 0 & 0 & 0 & 0 & 0 & 0 \\ -uv & v & u & 0 & 0 & 0 & 0 & 0 & 0 \\ K - v^2 & -u\Gamma & v(2 - \Gamma) & \Gamma & p\Gamma & -\Gamma & -\Gamma & -p\Gamma & 0 \\ v(K - H) & -uv\Gamma & H - v^2\Gamma & v(\Gamma + 1) & vp\Gamma & -v\Gamma & -v\Gamma & -vp\Gamma & 0 \\ -\varphi v & 0 & \varphi & 0 & v & 0 & 0 & 0 & 0 \\ \varphi v\mathcal{B} & 0 & -\varphi\mathcal{B} & 0 & 0 & v & 0 & 0 & 0 \\ -\chi v & 0 & \chi & 0 & 0 & 0 & v & 0 & 0 \\ 0 & 0 & 0 & 0 & 0 & 0 & 0 & v & 0 \\ 0 & 0 & 0 & 0 & 0 & 0 & 0 & 0 & v \end{bmatrix},$$

where $\Gamma = (\gamma - 1)/(1 - b\rho)$, $K = \Gamma(u^2 + v^2)/2$, $H = E + (p/\rho)$, $\varphi = b/(\gamma - 1)$, and $\chi = a\rho(4 - 2\gamma - 3b\rho)/(\gamma - 1)$.

It is interesting to note that in the current two-phase (liquid-gas) flow application, we may simplify our model system by replacing (2.5d) and (2.5e) with the single transport equation for the volume fraction of the liquid,

$$\frac{\partial Y}{\partial t} + u \frac{\partial Y}{\partial x} + v \frac{\partial Y}{\partial y} = 0,$$

$Y \in [0, 1]$, and then set the material quantities γ and a based on the expressions,

$$\gamma = 1 + 1 \left/ \left[\frac{Y}{\gamma^{(l)} - 1} + \frac{1 - Y}{\gamma^{(g)} - 1} \right] \right., \quad a = Y a^{(l)} + (1 - Y) a^{(g)},$$

where $\gamma^{(l)}$, $a^{(l)}$, and $\gamma^{(g)}$, $a^{(g)}$ are the polytropic and van der Waals gas constant for the liquid and gas, respectively. This latter formulation of the model equations has the advantage that is robust for problems when both the set of governing equations and the type of equations of state are different from one fluid component to the others, separated by the interfaces, see [11, 13] for an example.

3. Numerical Results. We use the high resolution method based on a wave-propagation viewpoint to compute approximate solutions of our multicomponent model introduced in Section 2. The method is a Godunov-type scheme in that we solve the Riemann problems in directions normal and tangential to each cell interface, and propagate the resulting waves (*i.e.*, discontinuities moving at constant speeds) to update the solutions in neighboring grid cells. Similar to many state-of-the-art shock capturing methods, high resolution version of the method can be achieved with the inclusion of slopes and limiters. Since the algorithmic details of this approach has been described fully before, see [10], it will not be repeated here.

We now apply our multicomponent algorithm to a model problem of shock waves in bubbly liquids. In this test, we take a shock tube of size $[-0.5, 1.5] \times [0, 1]$ m², and consider a planarly rightward-moving Mach 1.7 shock wave in liquid with data in the preshock state as

$$(\rho, u, v, p)_{\text{preshock}}^{(l)} = (10^3 \text{ kg/m}^3, 0, 0, 10^5 \text{ Pa}),$$

and data in the post-shock state as

$$(\rho, u, v, p)_{\text{post-shock}}^{(l)} = (1.196 \times 10^3 \text{ kg/m}^3, 404.84 \text{ m/s}, 0, 10^9 \text{ Pa}).$$

The equation of state parameters we employed for the liquid are $\gamma = 7$ and $\mathcal{B} = 3 \times 10^8 \text{ Pa}$. In addition to the shock wave, we assume that there is an array of gas bubbles of radius $r_0 = 3 \text{ cm}$ each which are distributed somewhat randomly with the minimum inter-bubble distance of 0.166m just below the shock, and some of them are about to be in contact with the shock, see Fig. 1.1 for an illustration of the problem setup. Here the gas volume fraction of the problem is 3.65%. Inside the gas bubble, the state variables are set by

$$(\rho, p, \gamma, a, b)_{\text{gas}}^{(g)} = (1.2 \text{ kg/m}^3, 10^5 \text{ Pa}, 1.4, 10^{-3} \text{ m}^3/\text{kg}, 5 \text{ Pa m}^6/\text{kg}).$$

Note that because of the large pressure jump across the shock wave, and also the large ratio of the acoustic impedances of the liquid to gas, $(\rho c)^{(l)}/(\rho c)^{(g)} \approx 3536$, this is a severe test for our multicomponent approach.

Figure 3.1 and 3.2 show sample results for a run using a 400×200 grid and the high-resolution version of the algorithm. From Fig. 3.1, complicated wave patterns after the passage of the shock wave to the bubbles are clearly observed, where contours of the pressure and volume fraction of the gas (introduced in the computation for monitoring the evolution of the gas bubbles) are presented at five different times $t = i/5 \text{ ms}$, for $i = 1, 2, \dots, 5$. The cross section of the results for the same run along line $y = 1/2 \text{ m}$ is drawn in Fig. 3.2, giving some quantitative information about the density, pressure, and temperature at the selected times.

To see how the time history of the maximum pressure of the problem changes as the strength of the incident shock wave is varied, we perform a comparison test with four different Mach numbers: 1.00085, 1.0094, 1.09, and 1.422, which correspond to $\mu = p_{\text{post-shock}}/p_{\text{preshock}} = 10^j$, for $j = 1, 2, 3, 4$. The result is shown in Fig. 3.3. It is clear that the behavior of the pressure become more and more dispersive as the strength of the incident shock is increased, but is more and more dissipative otherwise. Note that in the figure, we have also included results for a similar run using a different set of material constants for the liquid; $\gamma = 4.4$ and $\mathcal{B} = 6 \times 10^8$, observing qualitatively the same structure of the solutions. Some works are in progress to validate this result as in comparison with the existing mathematical theories of a ‘‘homogenized’’ version of the problems (cf. [1, 2]).

ACKNOWLEDGEMENT

This work was supported in part by National Science Council of Republic of China Grant NSC-87-2115-M-002-016.

REFERENCES

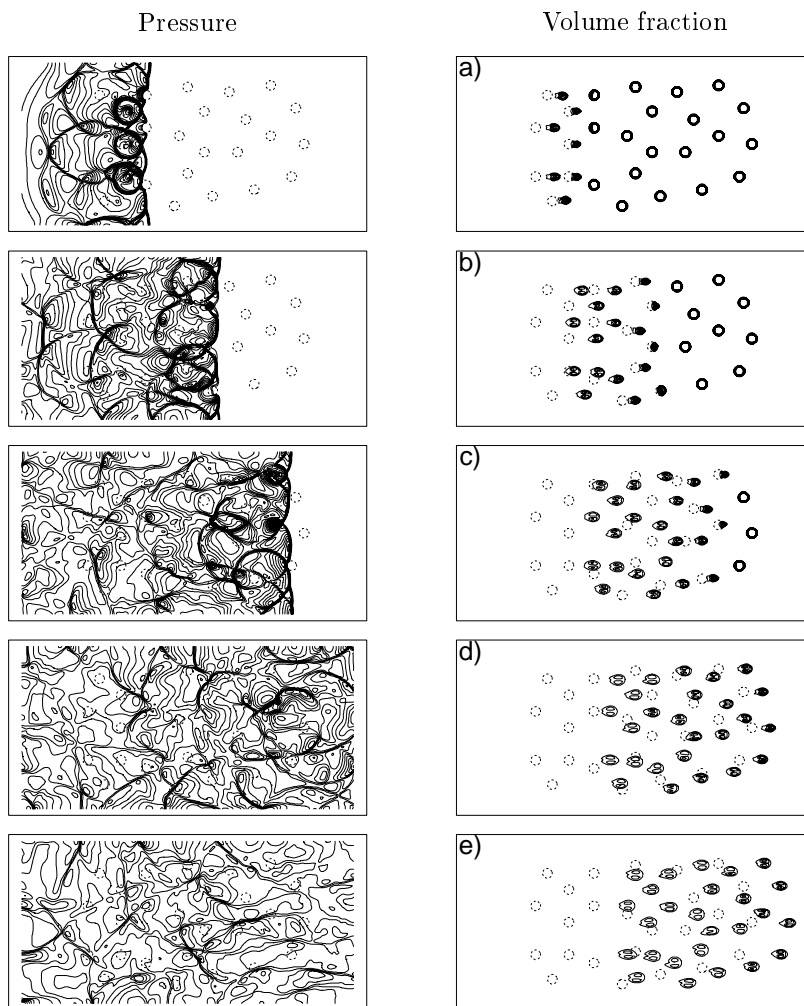


FIG. 3.1. High resolution results for a planar Mach 1.7 shock wave in liquid over an array of gas bubbles. Contours of the pressure and the volume fraction of the gas are shown at five different times: (a) at time $t = 0.2\text{ms}$, (b) at time $t = 0.4\text{ms}$, (c) at time $t = 0.6\text{ms}$, (d) at time $t = 0.8\text{ms}$, (e) at time $t = 1\text{ms}$. The dashed lines in the plots are the initial location of the gas bubbles.

- [1] R. E. Caflisch, M. J. Miksis, G. C. Papanicolaou, and L. Ting. Effective equations for wave propagation in bubbly liquids. *J. Fluid Mech.*, 153:259–273, 1985.
- [2] R. E. Caflisch, M. J. Miksis, G. C. Papanicolaou, and L. Ting. Wave propagation in bubbly liquids at finite volume fraction. *J. Fluid Mech.*, 160:1–14, 1985.
- [3] E. L. Carstensen and L. L. Foldy. Propagation of sound through a liquid containing bubbles. *J. Acoust. Soc. Am.*, 19:481–501, 1947.
- [4] J. D. Cheeke. Single-bubble sonoluminescence: bubble, bubble, toil and trouble. *Can. J. Phys.*, 75:77–96, 1997.
- [5] R. Courant and K. O. Friedrichs. *Supersonic Flow and Shock waves*. Wiley-Interscience, New York, 1948.
- [6] D. R. Lide. *Handbook of Chemistry and Physics*. CRC Press, 76 edition, 1996.
- [7] S. P. Marsh. *LASL Shock Hugoniot Data*. University of California Press, Berkeley, 1980.
- [8] R. I. Nigmatulin. *Dynamics of Multiphase Media*. Hemisphere, New York, 1991.
- [9] K.-M. Shyue. An efficient shock-capturing algorithm for compressible multicomponent problems. *J. Comput. Phys.*, 142:208–242, 1998.

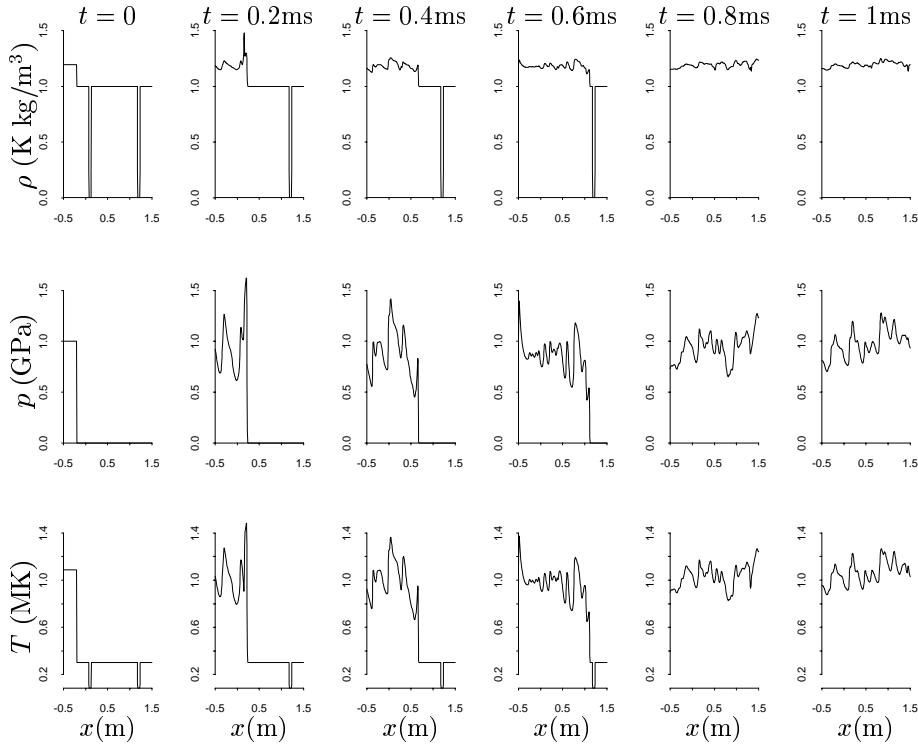


FIG. 3.2. Cross-sectional plots of the density, pressure, and temperature for the run performed in Fig. 3.1 along $y = 1/2\text{m}$ are shown.

- [10] K.-M. Shyue. A fluid-mixture type algorithm for compressible multicomponent flow with van der Waals equations of state. *J. Comput. Phys.*, submitted for publication, 1998. Available on the web: <http://www.math.ntu.edu.tw/shyue/vwaal.ps.gz>.
- [11] K.-M. Shyue. *An Eulerian interface-capturing approach for compressible two-phase flow with van der Waals-type fluids*. Final report: NSC87-2115-M-002-016, National Science Council, Taiwan, R.O.C., 1998 (unpublished). Available on the web: <http://www.math.ntu.edu.tw/shyue/2phase.ps.gz>.
- [12] K.-M. Shyue. Direct numerical simulations of shock waves in bubbly liquids. *In preparation*, 1999.
- [13] K.-M. Shyue. A volume-of-fluid type algorithm for compressible two-phase flows. In *Hyperbolic Problems: Theory, Numerics, Applications*, pages 895–904. Birkhäuser-Verlag, 1999. Intl. Series of Numerical Mathematics, Vol. 130.
- [14] M. J. Tan and S. G. Bankoff. Strong shock waves propagating through a bubbly mixture. *Experiments in Fluids*, 2:159–165, 1984.
- [15] L. van Wijngaarden. One-dimensional flow of liquids containing small gas bubbles. *Ann. Rev. Fluid Mech.*, 4:369–394, 1972.
- [16] M. Watanabe and A. Prosperetti. Shock waves in dilute bubbly liquids. *J. Fluid Mech.*, 274:349–381, 1994.

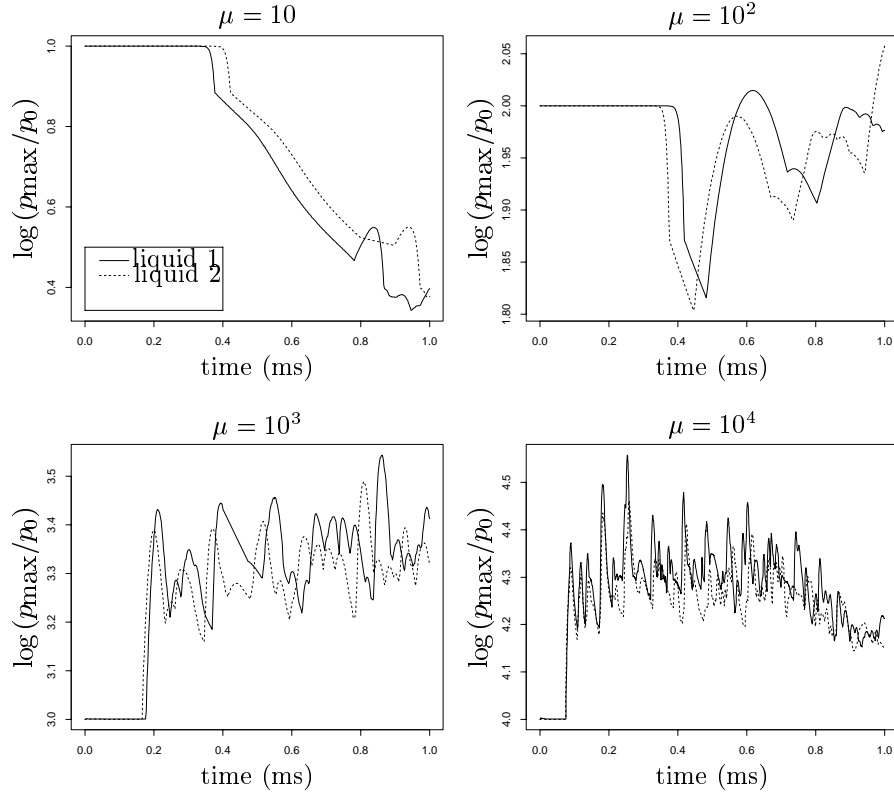


FIG. 3.3. Comparison of the maximum pressure history for a model of shock waves in bubbly liquids with different wave strength μ and material constants γ and B for the liquid. Note that for liquid 1, we have used $(\gamma, B) = (7, 3 \times 10^8 \text{ Pa})$, while for liquid 2, $(\gamma, B) = (4.4, 6 \times 10^8 \text{ Pa})$.